the plant journal

SEB Society for Experimental Biology

The Plant Journal (2016) doi: 10.1111/tpj.13425

TECHNICAL ADVANCE

High-throughput physiological phenotyping and screening system for the characterization of plant–environment interactions

Ofer Halperin[1], Alem Gebremedhin[2], Rony Wallach[1] and Menachem Moshelion[2,*]

[1]*Department of Soil and Water Sciences, The Robert H. Smith Faculty of Agriculture, Food and Environment, The Hebrew University of Jerusalem, Rehovot 76100, Israel, and*

[2]*The Robert H. Smith Institute of Plant Sciences and Genetics in Agriculture, The Robert H. Smith Faculty of Agriculture, Food and Environment, The Hebrew University of Jerusalem, Rehovot 76100, Israel*

Received 14 November 2014; revised 3 November 2016; accepted 7 November 2016.
*For correspondence (e-mail menachem.moshelion@mail.huji.ac.il).

SUMMARY

We present a simple and effective high-throughput experimental platform for simultaneous and continuous monitoring of water relations in the soil–plant–atmosphere continuum of numerous plants under dynamic environmental conditions. This system provides a simultaneously measured, detailed physiological response profile for each plant in the array, over time periods ranging from a few minutes to the entire growing season, under normal, stress and recovery conditions and at any phenological stage. Three probes for each pot in the array and a specially designed algorithm enable detailed water-relations characterization of whole-plant transpiration, biomass gain, stomatal conductance and root flux. They also enable quantitative calculation of the whole plant water-use efficiency and relative water content at high resolution under dynamic soil and atmospheric conditions. The system has no moving parts and can fit into many growing environments. A screening of 65 introgression lines of a wild tomato species (*Solanum pennellii*) crossed with cultivated tomato (*S. lycopersicum*), using our system and conventional gas-exchange tools, confirmed the accuracy of the system as well as its diagnostic capabilities. The use of this high-throughput diagnostic screening method is discussed in light of the gaps in our understanding of the genetic regulation of whole-plant performance, particularly under abiotic stress.

Keywords: phenotyping plant stress response, whole-plant water relation, transpiration, root flux, soil–plant–atmosphere continuum, genotype-by-environment interaction, functional phenotyping, technical advance.

INTRODUCTION

Modern sequencing technologies have dramatically reduced the time and expense of whole-genome sequencing. Consequently, many crop genomes have become available, providing valuable information on crop-related characteristics (traits) such as fruit ripening, grain traits and flowering-time adaptation (Bolger *et al.*, 2014). However, and despite enormous effort, the identification of higher levels of tolerance to different types of abiotic stress lags behind (Graff *et al.*, 2013), as abiotic-stress-tolerance traits are difficult to find. This is due to the complex nature of the phenotype, the number of genes involved and the presence of strong genotype-by-environment interactions (Richards *et al.*, 2010). Therefore, fast and accurate phenotyping remains a bottleneck in the effort to enhance yields in water-limited and other stressful environments (Richards *et al.*, 2010; Moshelion and Altman, 2015).

There are two occasionally overlapping uses of phenotypic information: to enhance our understanding of the functional significance of particular genes or gene clusters (termed diagnostic tool in this paper), and to develop selectable markers for breeding programmes, such as robust molecular markers and easily measured morphological, developmental or physiological characteristics (Passioura, 2012). The development of phenotype-selection tools for use in dedicated high-throughput, controlled-environment facilities could potentially improve precision

while reducing the need for replication in the field. Such tools have heralded the age of 'phenomics' (Furbank and Tester, 2011).

Novel high-throughput selection systems have been developed to enable the rapid screening of large plant populations in controlled, pre-field environments. The aim of these systems is to identify individual plants showing improved behavior under particular conditions at an early stage of their life cycle, prior to the mandatory, large-scale field trials. To date, most of these methods have been based on noninvasive imaging, spectroscopy, image analysis, robotics and high-performance computing (Furbank and Tester, 2011). During such screens, different images of each plant are recorded and analyzed using sophisticated image-analysis algorithms (Golzarian *et al.*, 2011; Hartmann *et al.*, 2011). Furbank and Tester (2011) described phenomics as 'high-throughput plant physiology'. In reality, the major physiological parameters reported by these systems are associated with plant size. This intrinsic property provides a good indication of the plant's growth rate and development under optimal growing conditions. However, under water limiting conditions, the first symptoms of stress to appear in angiosperms are turgor loss and inhibition of cell growth, while the stomata remain open and the rate of photosynthesis continues to be relatively high. If the stress is prolonged, gradual stomatal closure and a reduction in photosynthetic rate will follow (reviewed by Hsiao and Acevedo, 1974; Taiz and Zeiger, 2010). Thus, at the onset of stress conditions, many plants show improved harvest indices (i.e., stomatal conductance and photosynthetic rate) and low levels of growth inhibition. Indeed, stomatal conductance has been shown to be a reliable indicator of the plant's response to stress (Munns *et al.*, 2010).

Future progress in crop breeding requires a new emphasis on plant physiological phenotyping for specific, well defined traits (Ghanem *et al.*, 2015). However, plants' dynamic responses to the environment (hourly to seasonally) are extremely hard to capture using manual physiological apparatuses. Weighing lysimeters (gravimetric systems) have been reported to be highly accurate in following changes in plant weight (Vera-Repullo *et al.*, 2015) and have been widely used for many years as a tool for irrigation applications due to their accurate detection of plant water-loss rates, soil water content (SWC), plant water use, and simulation of drought stress (Earl, 2003; Pereyra-Irujo *et al.*, 2012). The current study presents a different approach, which makes use of the gravimetric system combined with soil and atmospheric probes for a high-resolution, high-throughput diagnostic-screening platform, to: (i) select plants with desired physiological traits, and (ii) study whole-plant water relations and biomass gain. The selection is based on a plant's unique stress-response profile compared to all others in the array.

Despite the enormous effort invested in the development of plants that are resistant to abiotic stress, only minor progress has been made. This is in large part due to the complexity of the different traits involved, the fluctuating nature of environmental conditions, and bottlenecks in the selection process. The suggested relatively simple screening system could remove some of these bottlenecks.

RESULTS

Comparison of whole-plant water relations in multiple plants

Using the comparative multiple whole-plant diagnostic system (Figure 1 and Experimental procedures), we first defined a set of criteria and parameters for use in identifying physiological differences between different whole-plant water-regulation behaviors under different ambient conditions. Major differences were identified between the physiological characteristics of wild tomato (*Solanum pennellii*; hereafter, Penelli) versus cultivated tomato (*Solanum lycopersicum* cv. M82; hereafter M82) species.

Under well-irrigated conditions, M82 showed faster growth and higher transpiration rates than Penelli. Under drought conditions, the growth rate and cumulative transpiration of the M82 plants decreased much more quickly than those of the Penelli plants (Figure 2a,b). When the plants were exposed to drought, the higher transpiration rate of M82 led to a much more rapid reduction in SWC than in pots containing Penelli plants (Figure 2c). The higher transpiration rate and biomass gain of M82 resulted in significantly lower water-use efficiency (WUE) compared to Penelli (Figure 2d). The higher transpiration rate of M82 was related not only to its larger size, but also to more transpiration per unit leaf area, as the transpiration rate normalized to leaf area (E) was also higher than that of the Penelli plants under both control and drought conditions. The Penelli plants responded to drought with a sharper reduction in E than the M82 plants under similar SWC conditions (Figure 2e). Similar relative behavior was obtained when the plant's transpiration rate as well as the whole-canopy stomatal conductance, g_{sc}, was normalized to the plant's weight (plant biomass instead of leaf area; Figure S1). The greater risk-taking behavior of M82 plants (i.e., lower sensitivity of stomatal response to diminishing SWC) yielded a lower drought-resistance index (DRI) compared to the Penelli plants (Figure 2f). All measurements took ~2–3 h, when the plants reached desired SWC. In Figure 2(e), the data for M82 and Penelli were averaged as follows: 80% SWC (pot capacity) was taken 29 days after planting for both M82 and Penelli, i.e., the last day of pretreatment; as M82 and Penelli reached 45% SWC at different times, we took the measurements when each plant reached the SWC target. Atmospheric conditions on these days were similar.

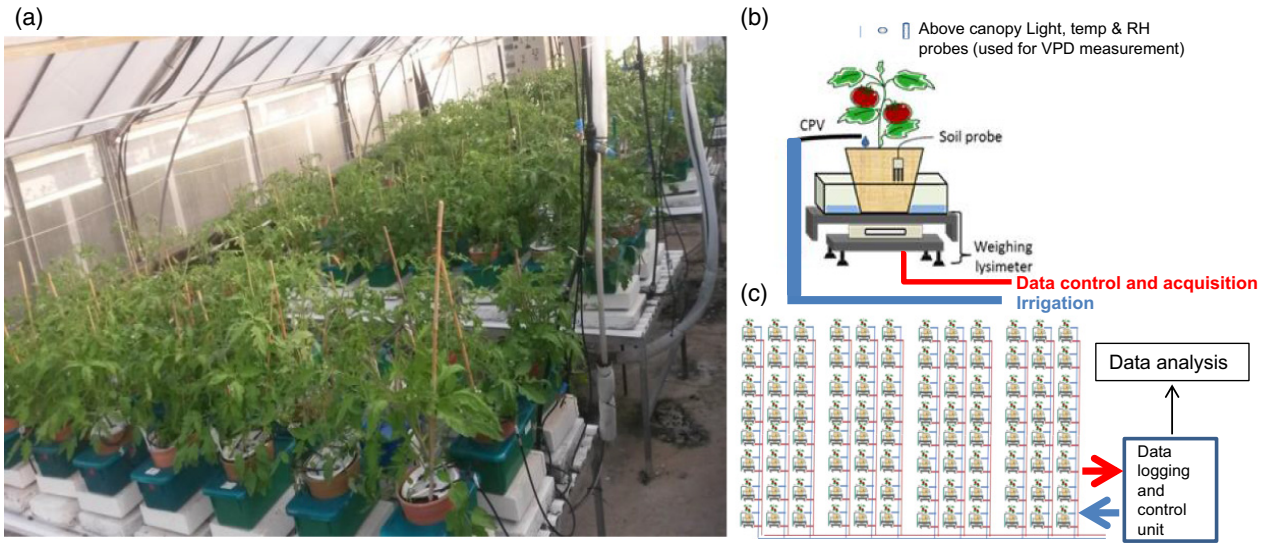

Figure 1. The lysimeter system.
(a) Top view of the greenhouse array (consisting of 96 weighing lysimeters) loaded with ILs, M82, MP1 and Penelli tomato plants. This fully automated system collects data from all of the units simultaneously.
(b) Drawing of a single unit composed of a 3.9-L pot inserted into an opaque plastic drainage container through an opening in the top of the container. The pot–container system sits on a sensitive temperature-compensated load cell. The purpose of the drainage container is to maintain water availability to the plant (0–600 ml) throughout the day to avoid weight changes caused by daytime irrigation events, which would complicate the calculation of continuous momentary transpiration rate. A soil probe in each pot continuously monitors the volumetric water content and electrical conductivity of the growth media. The irrigation system is controlled by preprogrammed valves (CPV) which are part of the control unit.
(c) A block diagram of the system composed of 96 units. The raw data output of the system can be seen in Figure S2. [Colour figure can be viewed at wileyonlinelibrary.com].

These physiological criteria were later used to examine the system's screening competence. All plants were placed on the lysimeter system at the same time and SWC was lowered gradually. A high degree of variability was observed in each of the physiological characteristics of the population (Figure S2). The Penelli plants were located at the boundaries and M82 and cultivated *S. lycopersicum* cv. MP1 (MP1 hereafter) around the middle of the distribution range of the physiological characteristics (Figure 3). Interestingly, many introgression lines (IL; Eshed and Zamir 1995) showed transgression, as they presented higher values than their parent lines (Figure 3). The measured parameters were sorted in panels from low to high values, allowing easy comparison for each measured parameter across all lines (Figure 3).

A comparison of the relative position-swap of each line between the first and second panels (Figure 3a,b, respectively) provides its relative WUE. Thus, plants with higher WUE levels are located higher on the growth-rate panel (Figure 3a, i.e., fast growing), and relatively lower on the cumulative transpiration panel (Figure 3b; e.g., line MP1) and vice versa (e.g., IL5-5). An additional qualitative parameter can be drawn from the relative shift in position between the second and third panels [i.e., position-swap between whole-plant transpiration (Figure 3b) and its relative position on the plot of transpiration normalized to leaf area (g_{sc}, Figure 3c)]. Here, we did not expect to see any substantial change between the panels. Nevertheless, the sharp shift to the right of IL6-2 and IL6-2-2, from the right end of the panel in Figure 3(b) to the left end of the panel in Figure 3(c), might indicate a stomatal control malfunction. Indeed, both genetically similar lines have a very low DRI (Figure 3d) and strong wilting phenotype (Figure 4). Interestingly, not all genetically similar IL plants presented similar phenotypes. For example, IL10-2 and IL10-2-2 exhibited very different physiological phenotypes [i.e., were positioned far from one another on the panels in Figure 3 and exhibited very different DRI values and corresponding morphology (Figure 4)].

These results revealed the system's ability to screen a large population for their physiological characteristics and pinpoint a small number of plants with the desired behavior (with good agreement to measurements reported in the literature; Table S1). However, to better understand the plants' different behaviors, high-resolution characterization is needed.

To test the system's diagnostic and plant-by-environment optimization capabilities, a detailed (high-resolution) comparative study was conducted for the two cultivated crop lines (M82 and MP1). These lines were chosen because they present similar behaviors, with MP1 exhibiting slightly higher growth and transpiration rates (Figure 3). This relative similarity allowed us to test the system's sensitivity and limitations.

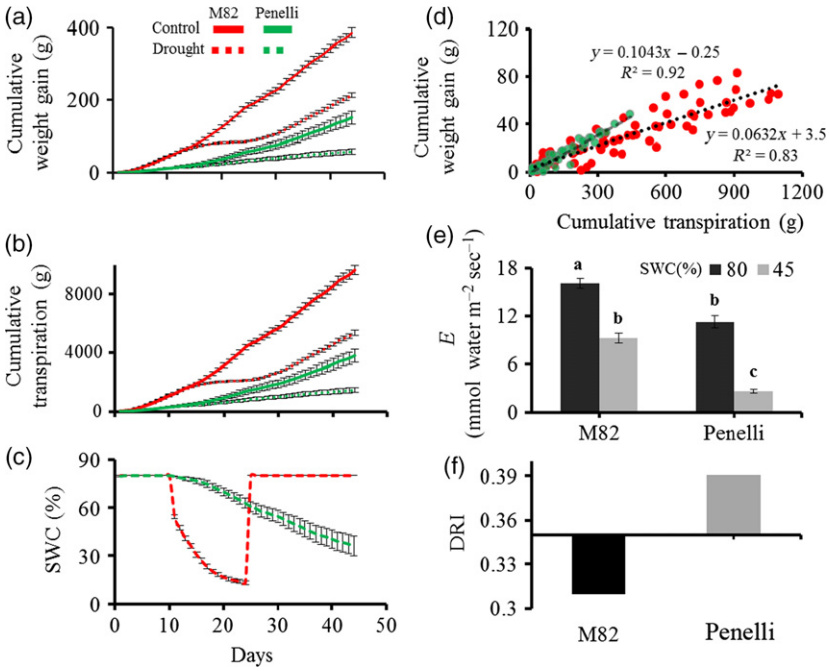

Figure 2. Comparison of the whole-plant drought responses of cultivated *Solanum lycopersicum* (M82) and green-fruited wild-type *S. pennellii* (Penelli) plants. M82 (red) and Penelli (green) plants were grown on the lysimeter system in a greenhouse (see Experimental procedures) with a period of full irrigation (10 days), followed by a drought treatment. Plants were irrigated again (recovered) when the soil reached 15% of soil water content (SWC).
(a) Mean daily cumulative weight gain ± SE of control (well irrigated throughout the whole period; solid lines) and drought-treated (dotted lines) plants.
(b, c) (b) Mean daily cumulative transpiration ± SE, and (c) mean SWC ± SE were measured continually for 45 days (SE bars are shown once every 5 days for clarity).
(d) The relationship between mean daily cumulative weight gain and transpiration throughout the first 10 days of the well-irrigated treatment. The slope of the lines indicates water-use efficiency (WUE). Slopes values are significantly different (Student's *t*-test, $P < 0.05$).
(e) Mean ± SE whole-plant midday transpiration rate at 80 and 45% SWC. A 76% decrease in *E* was observed among the Penelli plants, and a 43% decrease among the M82 plants.
(f) Drought-resistance index (DRI, see Experimental procedures). Different letters above columns represent significant differences (two-way ANOVA: Tukey–Kramer, $P < 0.05$, n = minimum of six plants from each line per treatment).

Comparison of mean whole-plant daily transpiration and stomatal conductance rates

The tests were conducted on several biological repeats of M82 and MP1 in an attempt to get statistically significant results. Here, as before, all plants were placed in the array and tested simultaneously.

The measured whole-plant transpiration rate (*E*) and canopy vapor conductance (g_{sc}) for a broad range of SWC values (Figure 5) yielded consistently higher values for MP1 versus M82. Repeating the experiment during the winter [similar vapor-pressure deficit (VPD) in the greenhouse, but ~30% less radiation due to natural light conditions, see Figure S3 and Experimental procedures], yielded lower maximum *E* and g_{sc} values with a similar behavior pattern among the plants and the plants' responses to the different environmental conditions. Note that the daily peak in canopy stomatal conductance), g_{sc} (Figure 5e), was reached ahead of the daily peak in VPD (Figure 5a). Both peaks were shifted toward the late morning hours during the winter experiment (Figure S3). The daily g_{sc} patterns represent the stomata's response to the ambient conditions (i.e., stomatal g_s is higher under low VPD conditions and decreases as VPD increases, assumed to prevent leaf desiccation. This daily stomatal behavior pattern is known from the literature (e.g., Brodribb and Holbrook, 2004), but its manual measurement is tedious work that requires major effort and is limited in the number of plants that can be measured simultaneously. In addition, the accuracy of our measurements were confirmed by gas-exchange apparatuses used to simultaneously measure a few more control M82 plants grown in parallel to the plants on the lysimeters, which yielded similar absolute values (see Experimental procedures and Figure S4).

Comparison of the temporal change in SWC, *E* or g_{sc} for many plants might be misleading because SWC depletion by plants that transpire more is higher than for those that transpire less, and the former will experience dry soil conditions at an earlier stage. Thus, presenting *E* versus SWC (Figure 6) seems more appropriate and has more

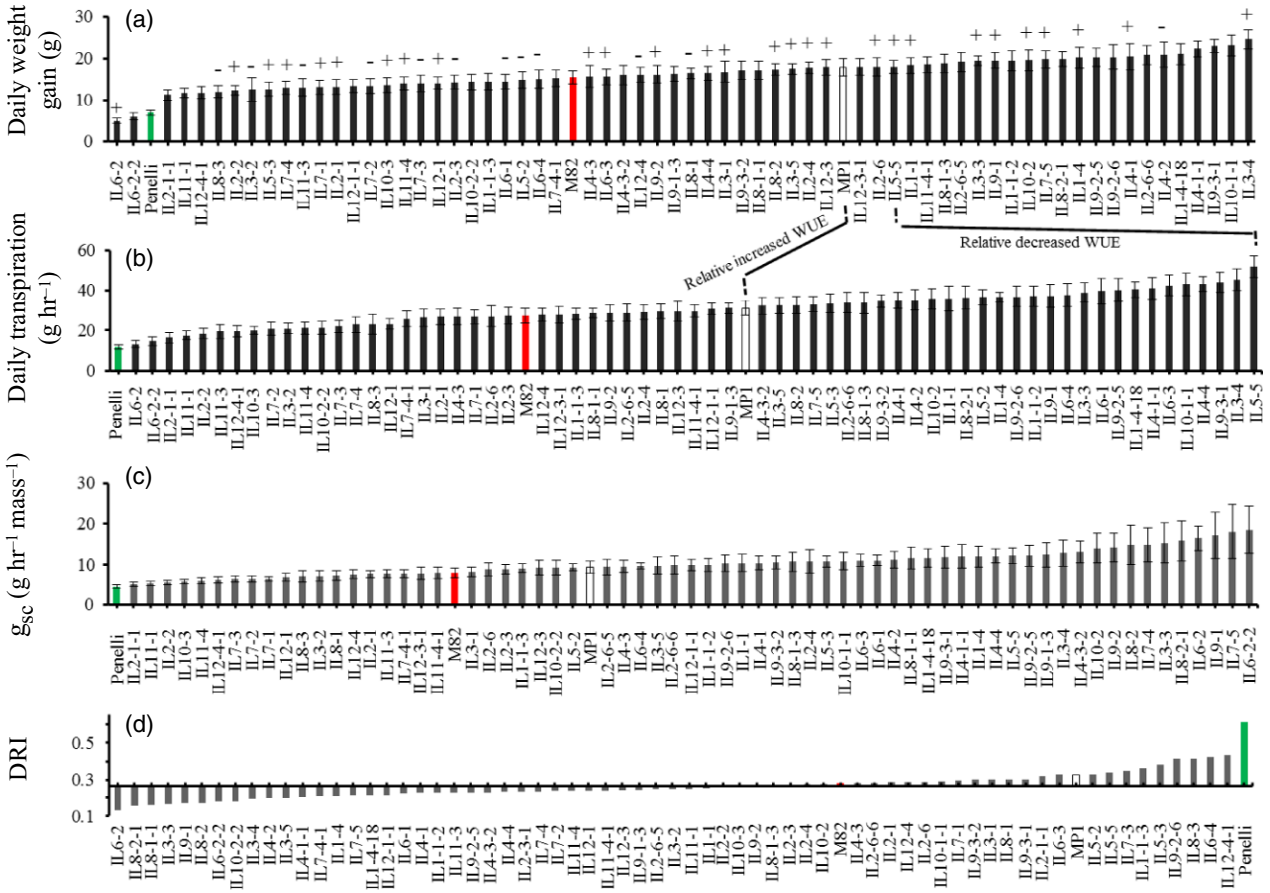

Figure 3. Ranked physiological characteristics of tomato population.
(a–d) ILs (black bars), M82 (red bars), Penelli (green bars) and additional cultivated tomato cv. MP1 (open bars) were grown on the lysimeter system under periodic intervals of full irrigation and drought. All plants were continuously monitored for: (a) daily whole-plant weight gain; + and − signs above the bars indicate match or mismatch, respectively, of plant weight relative to field-grown plants, as culled from the literature (see Table S1), revealing 72% agreement between our measurements and those reported in the literature, (b) daily whole-plant midday transpiration; plant's relative WUE could be concluded based on the angle of its position-shift for MP1 and IL5-5, (c) whole-plant midday canopy stomatal conductance (g_{sc}); plant weight was obtained from the lysimeter system, (d) drought-resistance index (DRI). Each column is the mean of five consecutive days from a single plant ± SE.

physiological relevance when transpiration regulation in different plants is being examined.

Relationship between whole-plant transpiration and SWC

The plot of midday transpiration level (*E*) versus SWC (Figure 6) showed that *E* remains constant for a wide range of SWCs under the given ambient conditions (E_{max}) and starts to decrease sharply at a certain SWC, denoted as critical soil water content (SWC_{cr}). The decrease in *E* beyond SWC_{cr} is linear, indicating that SWC becomes a limiting factor for plant transpiration. Note that this conclusion is reinforced by the fact that ambient conditions were similar throughout the drought-treatment period (Figures 5a and S3a). The *E* of MP1 was consistently higher than that of M82 across the range of examined SWC levels and light conditions during both summer (Figure 6a) and winter (Figure 6b) experiments. Note that while the summer and winter experiments differed with respect to level of natural irradiance, the winter VPD was maintained similar to the summer VPD by artificial means (Figures 5a and S3a).

When soil water is fully available, the plant's ability to convey and transpire water depends on its physiological, morphological and anatomical characteristics, forming an inherent E_{max} (Figure 6c). A comparison of stomatal densities and apertures of MP1 and M82 revealed similar stomatal densities (24 ± 3 and 21.3 ± 1.3 stomata per 0.1 mm^2 for MP1 and M82, respectively, mean ± SE, *n* = at least 16 leaves per line) and significantly wider stomatal apertures for MP1 versus M82 (45.5 ± 1.6 μm^2 and 25.2 ± 2 μm^2, respectively, mean ± SE, *n* = at least 16 leaves per line) in the presence of similar soil–atmosphere water-potential differences. Therefore, one might conclude that in the presence of similar environmental signals, the sensitivity of the M82 stomatal response is greater than that of MP1,

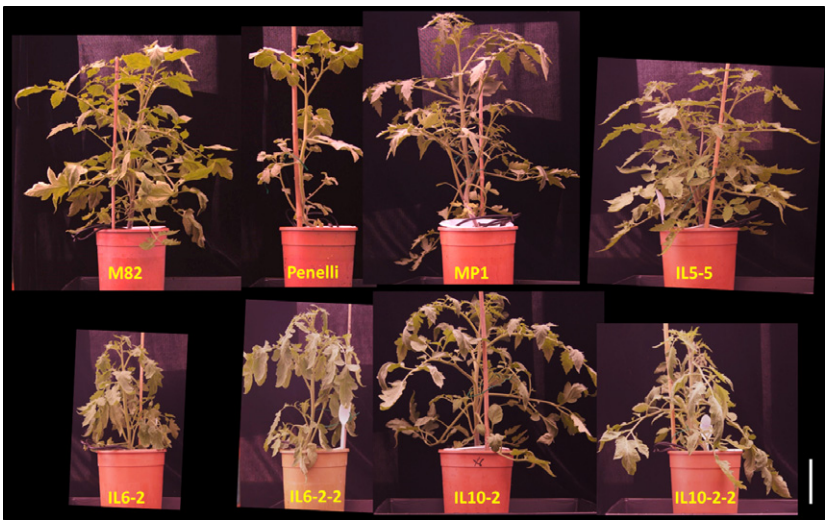

Figure 4. Plants (39 days old) of cultivated tomato *Solanum lycopersicum* cv. M82, cv. MP1, the wild-type tomato *Solanum pennellii* and a few more selected ILs (see text for explanation).
The pictures were taken at the end of the pretreatment phase of the experiment. Bar = 10 cm. [Colour figure can be viewed at wileyonlinelibrary.com].

with M82 exhibiting more conservative water-balance management behavior.

Whole-plant root-to-shoot water flux and relative water content (RWC)

An additional important feature of the current screening system is the continuous whole-plant water-balance phenotyping evaluated by simultaneous measurement of the rates of water flow into the roots (J_r) and out of the canopy (ET; Figure 7). J_r is evaluated by continuously measuring SWC (using soil probes, Figures 1 and 5) and ET by continuously measuring lysimeter weight (see Experimental procedures). The continuous measurement of ET and J_r provides a view of the temporal difference between the two fluxes and their variation over time. The difference between the water inflow and outflow is considered a measure of the variation of the whole-plant relative water content (RWC_{plant}). Differences between the two fluxes indicate that RWC_{plant} is either decreasing or increasing (Figure 7c and Experimental procedures). In general, water outflow was higher than inflow for both lines during the early morning hours. Equilibrium between inflow and outflow was reached in the late morning hours and persisted through midday. Water inflow became higher than the outflow during the afternoon hours (Figure S5). The comparison between the daily RWC_{plant} patterns for MP1 and M82 plants indicated a greater daily RWC_{plant} gain for MP1 at 40–50% SWC (Figure 7c). However, under severe stress, MP1 plants experienced greater RWC_{plant} loss than M82 plants. These observations were congruent with the manual leaf RWC measurements and the growth-rate patterns of these lines (Figures S6 and S7a, respectively). There was a high correlation between the daily transpiration and root water-uptake rates (Figure 8). Furthermore, the positive slope of the fitted line expressed the plant's daily weight gain.

DISCUSSION

The predominant procedure for developing new crop cultivars is based on selection of a few plants out of thousands using conventional field-based selection criteria that require whole seasons and repeated large-scale field trials. This can take several years and a great deal of resources, with a limit on the number of promising candidates that can be simultaneously screened (Moshelion and Altman, 2015). Soil-drying experiments can at first seem quite straightforward, but often turn out to be some of the most difficult to interpret (Verslues *et al.*, 2006). Here, we demonstrate a noninvasive, high-throughput physiological phenotyping and screening system which can easily be integrated in research and development programs aimed at optimizing genotype-by-environment interactions at pre-field phases of breeding programs or characterizing plant nutrition, or in basic plant physiology research, among others.

Screening by the current system can provide for comparative examination and graded ranking of different physiological characteristics [i.e., growth rate, WUE, DRI, ET, E, g_{sc}, J_v, RWC_{plant}] or elucidation of the relations between characteristics among an entire population (as the system can be easily scaled up to much greater numbers of units, a large germplasm population can be screened as well). The screening can be performed for different ambient conditions and a variety of plant phenological stages. The relative difference between the values of each of the parameters for optimal versus stress conditions can be quantified as individual stress index (e.g., Figure 2f). Plant resilience can also be easily evaluated by this system as the rate at which plants recover from stress after returning to a well-irrigated regime, with faster recovery indicating a more resilient plant (Figure S7b). Obviously, any combination of plant characteristics under different treatments and

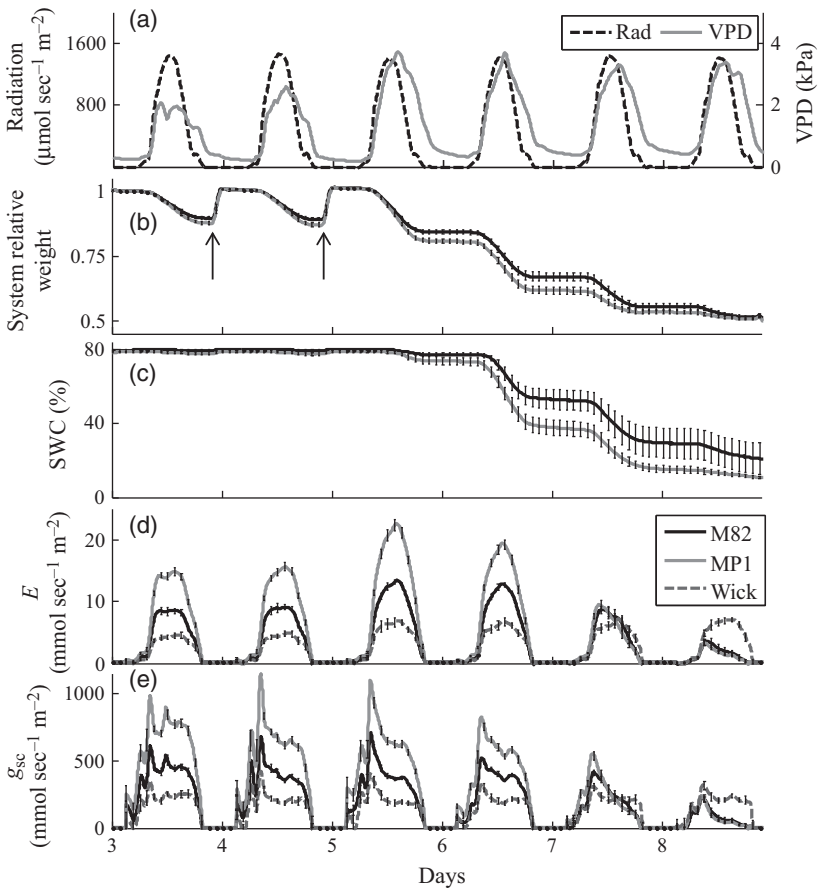

Figure 5. Variation in different whole-plant parameters of M82 and MP1 plants along a soil–atmosphere water gradient.
(a) Daily VPD and radiation (Rad) over 6 consecutive days of the experiment, which included 3 days of full irrigation followed by 3 days of drought.
(b) Variation in plants' weights (relative to their respective initial weights) over the course of the full irrigation and drought treatments. The observed weight increase (marked by arrows) was the result of irrigating up to the level of the drainage hole.
(c) Variation in soil water content (SWC) over the 6 days of the experiment.
(d) Whole-plant transpiration (E) over the course of the experiment. To eliminate the effect of plant size on transpiration rate, we normalized the rate of plant water loss to the leaf surface area.
(e) Whole-plant canopy vapor conductance (g_{sc}) was calculated as the ratio of E to the simultaneously calculated VPD. Each curve (b–e) is the mean of 9–11 plants of each line; SE values were calculated every 90 min.

at different phenological stages can be used to construct a plant's water-relations management profile and its location in the population distribution.

The system's ability to simultaneously monitor a large number of plants at high temporal resolution using three sensors further enables evaluation of momentary variations in essential parameters (Figures 5–7), which can be used to screen related levels of performance. This detailed information, combined with the ability to apply different treatments to each plant, provides the researcher with a valuable comparative tool for selection, diagnosis and optimization (e.g., optimal growth × environment × management).

Decision-making: choosing the right plant for the right environment

Quantitative, objective and automated screening techniques and algorithms have many potential advantages, enabling rapid screening of the most promising crop lines at an early stage, followed by the necessary field trials. However, to become essential tools for predicting a desired trait, these methods must take into account the complex nature of the interactions between biological factors, management practices and environmental conditions. For example, whereas light and VPD control E_{max} when soil water is readily available, under lower SWCs, soil water availability becomes the limiting factor, inducing a decrease in transpiration (Figure 6). The gradual decrease in E observed when SWC decreases below SWC_{cr} indicates that for $SWC < SWC_{cr}$, E fails to meet the atmospheric water demand. Moreover, the value of SWC_{cr} depends, inter alia, on the momentary atmospheric water demand and decreases as E_{max} decreases (as was observed in the winter experiment, Figure 6). Moreover, stomatal conductance is known to be a reliable indicator of growth-rate responses to stress (reviewed by Munns *et al.*, 2010). Evaluation of g_{sc} together with variations in SWC provides an additional plant-by-environment selection characteristic.

The fine regulation of whole-plant water balance depends on many control points along the soil–plant–atmosphere continuum. For example, leaves will be at risk of dehydration if the amount of water lost by transpiration is greater than the amount of water uptake by the roots. This scenario is controlled by the combined effect of soil water availability and VPD as a measure of atmospheric water demand. Hence, one of the advantages of this system is the ability to measure the water-flux balance for individual plants in the array. As an example, our results revealed

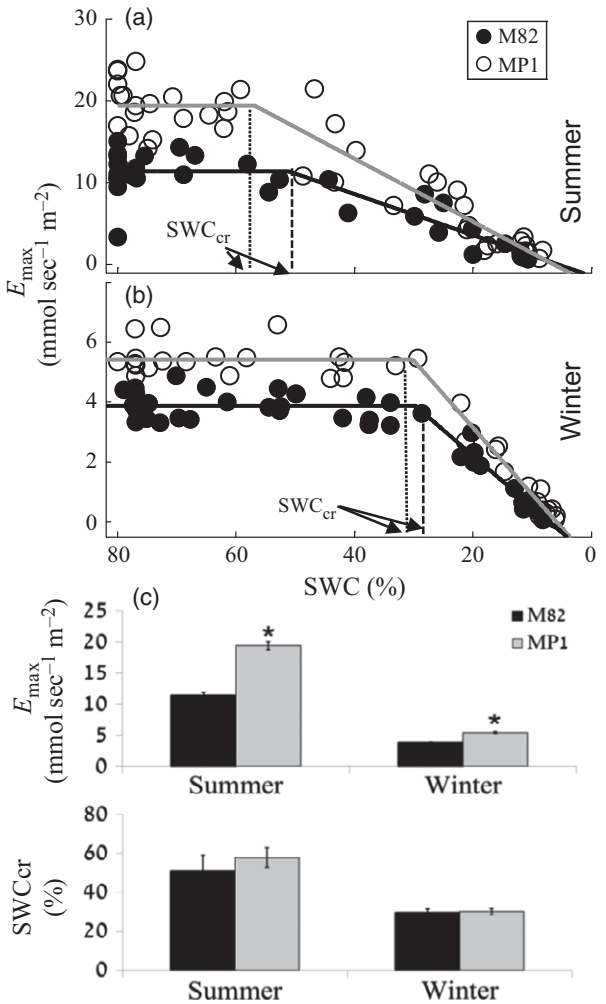

Figure 6. Midday transpiration versus soil water content (SWC).
(a, b) Midday whole-plant transpiration as a function of SWC over the entire period of (a) the summer experiment (same plants as in Figure 1) and (b) the winter experiment (n = 11 for MP1, n = 9 for M82; see Figure S2 for a description of the ambient conditions).
(c) Mean ± SE of the maximum daily transpiration rate (E_{max}) and mean ± SE critical soil water content (SWC_{cr}). Asterisks indicate no overlap in 95% confidence intervals.

that during the early morning hours, in both M82 and MP1, leaf water outflux exceeds the root water influx (Figures 7 and S5). This difference led to a leaf water deficit (i.e., reduced RWC at noon). The system's reliability was confirmed by conventional leaf RWC measurements (Figure S6). Moreover, the high correlation between plant root water uptake and transpiration rate for well-irrigated plants indicated that the soil-embedded sensor provides a reliable estimate of water flux to the plant's roots and confirms the RWC_{plant} determination as the balance between the two variables. Hence, comparison of Figures 7(c) and 8 indicates that the slightly larger than one slope in the latter is responsible for plant growth (RWC_{plant} > 100%) observed in the former during the second half of the day.

This momentary high-resolution comparison also enables the identification of relatively small differences among plants. For example, during the drought treatment, M82 plants maintained a flux balance similar to that observed under nonstress conditions. In contrast, in the MP1 plants, the water deficit increased (i.e., the difference became greater due to higher ET relative to J_r; Figure 7b), suggesting the existence of a different, less strict regulation mechanism in MP1 plants, resulting in more anisohydric behavior.

The changes in sensitivity of different plants' responses may have advantages under certain ambient conditions. The challenge is to evaluate the relative importance of each characteristic for plant performance in the field. For example, high DRI values (Figure 3d) might be a good survivability trait, but might not be considered important for crop production in environments with mild to moderate drought. In those types of environments, more risk-taking behaviors (i.e., higher g_s) might be considered better traits as they can lead to higher yields (Sade *et al.*, 2009, 2010; Moshelion *et al.*, 2014). Careful consideration of the desired traits with a view of expected stress scenarios is a crucial part of any breeding program.

CONCLUSIONS

The ability to select candidate plants exhibiting a superior stress-response strategy, in addition to other desirable traits, is essential for research and development of crops with the desired adaptation to environmental stress. We describe a simple, yet robust system that can be easily installed at any research and development facility. We expect that use of the relatively rapid screening protocol and equations detailed herein (which can be easily modified to fit any particular research program) will speed up the development process, and allow continuous measurement of the behavior of crop plants under nonstress and stress conditions. It is likely that initially, the major benefit of the screening will be the early elimination of candidates that are unlikely to perform well in trait-integration field trials performed under the expected environmental conditions. The diagnostic capabilities of this system are likely to be integrated later on into optimization procedures (i.e., plant adaptation to soils, nutrient composition, etc.), as well as basic plant physiology research, helping the researcher translate data into knowledge and decision-making tools.

EXPERIMENTAL PROCEDURES

Experimental setup

The experimental study was conducted in semi-commercial greenhouses at the Faculty of Agriculture, Food and Environment in Rehovot, Israel during December 2011 and June 2012 (referred to as winter and summer experiments, respectively). The

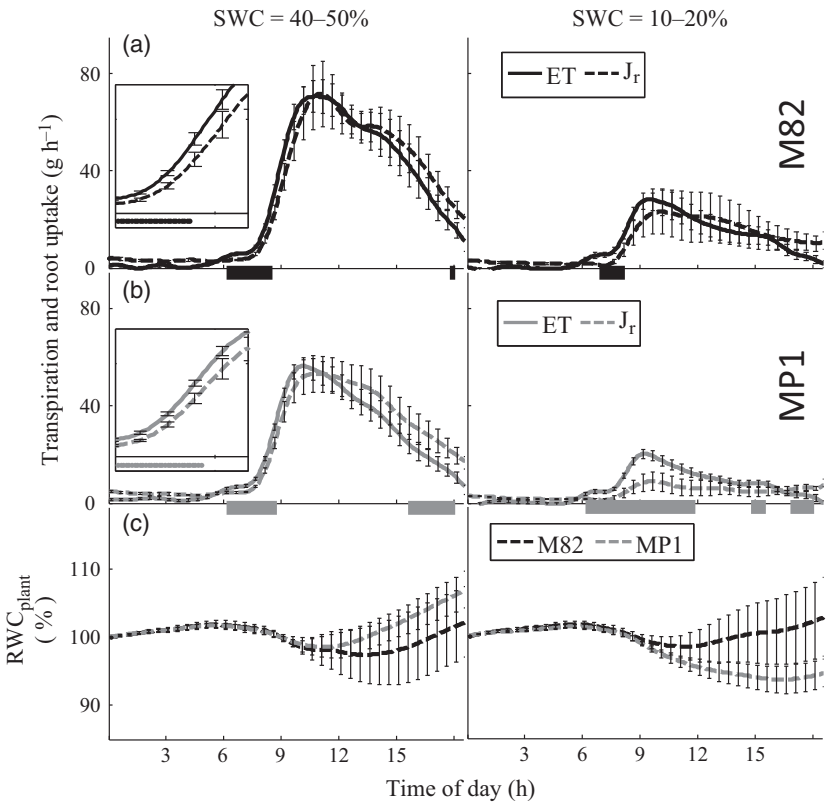

Figure 7. Daily water influx and outflux and whole-plant water balance at different soil water content (SWC) levels.
(a–c) Daily pattern of the rate of plant water loss (ET) and the rate of root water uptake (J_r) measured simultaneously for (a) M82 and (b) MP1. The cumulative difference between the influx and outflux is the change in (c) whole-plant relative water content (RWC_{plant}). Each data point is the mean ± SE of at least nine plants per line. Lines under the curves indicate a significant difference (Student's *t*-test, $P < 0.05$, every 30 min) between the transpiration rate and the rate at which water was taken up by the roots. Insets show the magnitudes of the slopes between 07:00 and 09:30 h.

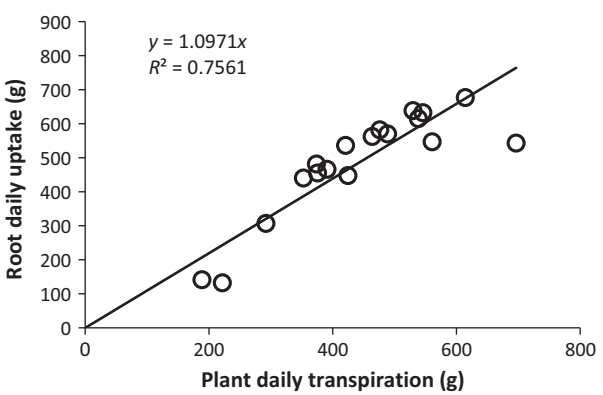

Figure 8. Comparison between amounts of water lost by transpiration and taken up by the roots in a single day (06:00–19:00 h) with soil water content of ~50% for all M82 and MP1 pots (each point represents a single pot).
A relatively high correlation between daily transpiration and root uptake was obtained for the entire range. The difference between transpiration and soil water uptake rates during the day could be attributed to plant weight gain.

experimental setup included 3.9-L growing pots placed on temperature-compensated load cells, referred to as lysimeters and gravimetric system (Tadea-Huntleigh, 1042 C4; Vishay Intertechnology, Malvern, PA, USA). The pots were filled with a commercial growing medium (Matza Gan, Shaham, Givat-Ada, Israel), composed of (w/w) 55% peat, 20% tuff and 25% puffed coconut coir fiber, with a mixture bulk density of 0.3 g cm^{-3}. Each pot was filled with 2.8 kg potting soil. The volumetric water content of the fully drained substrate, namely the pot capacity, was 80%. The growing medium is referred to as "soil." A single plant was grown in each pot. Each pot was immersed in a plastic container (13 × 21.5 × 31.5 cm H × W × L) through a hole in its top cover (Figure 1). Evaporation from the containers and pots was prevented by a plastic plate cover, punched in the middle to allow the plant stem to emerge. Six wet wicks were placed on six additional load cells randomly distributed among the pots with plants. The wicks were made of a woven rag, the lower part of which was submerged in free water. The water loss from the wicks provided a reference for the effect of ambient conditions on transpiration.

Prior to the experiments, three random load cells were examined for reading accuracy, and in particular for drift level under constant weight-load. These measurements were performed for several days, and the results of two sequential representative days are depicted in Figure S8. No drift in the constant weight reading was observed. The periodic fluctuations of ± 3–4 g (~0.1%) in the load-cell reading that were induced by input voltage fluctuations of ±25 mV (0.25%). These small fluctuations are a result of temperature fluctuations in the greenhouse and noise that that is inherent to electronic systems.

In all experiments, 4- to 5-week-old seedlings (on the first day of the experiment) were used. The plants were sown in small (~50 ml) pots and transferred to the 3.9-L pot 3 weeks later, after careful washing of the roots, for an additional 10–14 days. The plants were grown under natural light conditions and vents blowing moist air to ensure that the maximum temperature in the greenhouse would not exceed 35°C. The temperature and relative humidity were, respectively, in the range of 25–35°C and 40–60% during the summer experiment and 18–35°C and 20–35% during the winter experiment. The temperature and relative humidity in

the greenhouse and the photosynthetically active radiation were monitored using an HC2-S3-L meteo probe (Rotronic, Crawley, UK) and LI-COR 190 Quantum Sensor (Lincoln, NE, USA). The weighing lysimeters, soil-moisture sensors and environmental sensors were connected a to a CR1000 data logger through AM16/32B multiplexers (Campbell Scientific, Logan, UT, USA). Readings of the weighing lysimeters and the environmental sensors were taken every 15 sec and averages for each 3-min period were stored in the data logger for further analysis. Soil moisture was measured every 3 min.

Each plant was irrigated by four on-surface drippers to ensure uniform water distribution in the pots at the end of the irrigation event and prior to free drainage. Plants were irrigated in three consecutive cycles, each consisting of 20 min watering followed by 40 min drainage, between 23:00 and 02:00. The daily pre-dawn pot weight was determined as the average weight between 05:00 and 05:30 h, after ensuring that drainage had ceased. After several days with an empty pot, very good repeatability was observed. The surplus water provided in each irrigation brought the water level in the containers underneath the pots at the end of the drainage event to 2 cm above the pot base. This water level was achieved by a drainage orifice in the container side wall through which the excess water drained. In addition to salt leaching from the pots, the excess irrigation ensured that water would be fully available to the well-irrigated plants throughout the following daylight hours without supplemental irrigation. The lack of additional irrigation throughout the daylight hours ensured a monotonic pot-weight decrease between subsequent irrigation events. This monotonicity enabled applying the data-analysis algorithm that was developed for this experimental setup. Moreover, reaching an *a priori* determined water level at drainage completion during the night enabled determining the daily plant weight gain. The procedure is detailed further on. A commercial fertilizer solution (Super Grow 6-6-6+3, Hortical, Kadima, Israel) was applied with the irrigation water at 0.2% (v/v) (fertigation).

A soil moisture, salinity and temperature sensor (5TE; Decagon Devices, Pullman, WA, USA) was embedded in each pot to provide time series for these three variables. The measured soil dielectric permittivity was converted to volumetric water content using a third-order polynomial (Topp *et al.*, 1980). The polynomial coefficients for the growing medium were determined experimentally. Greenhouse measurements of light and VPD before the start of the experiment were similar to the conditions reported in Figures 5 and S3 (for summer and winter experiments) respectively.

The experiment with ILs consisted of 5-week-old ILs ($n = 65$) of the wild tomato species (Penelli) against the background of the cultivated tomato M82, their parents, and the additional cultivated tomato MP1. The experimental study included two treatments: surplus irrigation and drought. The plants in the drought treatment were dehydrated by stopping irrigation.

The daily transpiration (PDT) of each plant was calculated as the difference between the load-cell readings pre-dawn (W_m) and in the evening (W_e) for each day:

$$\mathrm{PDT} = W_m - W_e \tag{1}$$

The values of W_m and W_e were determined as the average load-cell reading over a 30-min period: 15 min prior to and following the specified time. This averaging intends to eliminate the effect of temporal variation in ambient conditions (which occurred particularly at the morning and afternoon hours) and random noise that is associates any electronic and data-acquisition systems. The data averaging over 30 time span were found to be adequate.

Being controlled by an orifice in its wall, the water in the container was constant at the cessation of free drainage, independent of plant weight. This enabled determining the plant weight gain (fresh weight or biomass) at the end of irrigation and drainage for any desired period (day, week, etc.). The plant daily weight gain ($\Delta\mathrm{PW}_n$) between consecutive days was:

$$\Delta\mathrm{PW}_n = W_n - W_{n-1} \tag{2}$$

where W_n and $W_{n\text{-}1}$ are the container weights upon drainage termination on consecutive days, n and $n-1$. Following Eq. 2, the weight on day n is the sum of plant weight on day $n-1$ and the weight gain $\Delta\mathrm{PW}_{n\text{-}1}$

$$\mathrm{PW}_n = \mathrm{PW}_{n-1} + \Delta\mathrm{PW}_n \tag{3}$$

The whole-plant WUE during a defined period was determined by the ratio between the sum of the daily plant fresh-weight gain (ΔPW) and water consumed throughout this period:

$$\mathrm{WUE} = \frac{\sum \Delta\mathrm{PW}_n}{\sum \mathrm{PDT}_n} \tag{4}$$

The WUE for the whole plant (Eq. 4) replaces the commonly used physiological WUE determined as the ratio between the accumulated CO_2 molecules and evaporated H_2O, which is usually determined for leaf patches. The values calculated by Eq. 4 are compatible with integrated WUE, which is expressed as biomass accumulation or yield per unit of water used (Yoo *et al.*, 2009). Equation (5) was then used to determine plant weight gain throughout the drought period, when plants were not irrigated and the above procedure to calculate the plants' weight gain could not be applied:

$$\sum \Delta\mathrm{PW}_n = \mathrm{WUE} \cdot \sum \mathrm{PDT}_n \tag{5}$$

where WUE was calculated for the well-irrigated period (Eq. 4), and PDT_n is the measured daily water consumption throughout the drought period.

The momentary whole-plant transpiration rate WPT was calculated by multiplying the first derivative of the measured load-cell time series by -1, assuming that the plant's weight gain during the short time interval used to calculate the transpiration rate is negligible and that under stress conditions, changes in the plant WUE are minor and can be therefore neglected:

$$\mathrm{WPT}_k \equiv -\left(\frac{dW}{dt}\right)_k \approx -\frac{W_k - W_{k-1}}{t_k - t_{k-1}} \tag{6}$$

W_k and $W_{k\text{-}1}$ are the load-cell readings at time t_k and $t_{k\text{-}1}$, respectively. The momentary water flux into the plants roots was similarly calculated by:

$$(J_r)_k \equiv -\left(\frac{d(\mathrm{SWC})}{dt}\right)_k \cdot V_s \approx -\frac{\mathrm{SWC}_k - \mathrm{SWC}_{k-1}}{t_k - t_{k-1}} \cdot V_s \tag{7}$$

where SWC in a pot is measured by the soil-embedded 5TE sensor, and V_s is the soil volume in the pot. In general, a numerical derivative of a time series amplifies the system's intrinsic noise (load cell, data-acquisition system). The noise amplification increases as the sampling interval, t_k and $t_{k\text{-}1}$, decreases. This noise was reduced prior to the differentiation (Eqn 6 and 7) by smoothing the data time series using the Savitzky and Golay (1964) method with a 61-data-point filtering window and a fourth-order polynomial (Wallach *et al.*, 2010).

Given that the spatial water content and root distribution in the pot are nonuniform and thus, neither is water uptake, the accuracy of the water-uptake evaluation by a single sensor was evaluated by a comparison between the simultaneously measured

accumulated water uptake and transpiration rate during the daylight hours (Figure 7). The comparison provided a fairly good fit, especially for the major range of the cumulative water-loss/uptake values.

RWC_{plant} was determined as the balance between the plant's water outflux (transpiration) and influx (root water uptake) (Eqns. 6 and 7). A comparison between the amount of water taken up by the roots and that lost by transpiration during day 7 (06:00 to 19:00 h, when the SWC content was about 50%) is depicted in Figure 8, where each point represents a single pot. A relatively high correlation between daily transpiration and root uptake was obtained for the entire range. Referring to Figure 7, the agreement between the daily transpiration and root uptake rates was higher for days when both were higher.

The difference between the momentary transpiration and soil water-uptake rates during a single day could be attributed to the momentary changes in RWC_{plant}. The change in RWC_{plant} at a given time during the day relative to midnight of that day, when the RWC_{plant} is assumed to be 100%, was 1. Therefore, RWC_{plant} was calculated by:

$$(1 - \mathrm{RWC}_n)*100 = \Delta\mathrm{RWC}_n = \frac{\sum_{n=0}^{n}(J_{r_n} - \mathrm{ET}_n)*\Delta t}{\mathrm{PW}} \quad (8)$$

where Δt is the sampling time interval (0.05 h in the current study), and n determines the time during the day. *PW* is the plant weight on the day for which RWC_{plant} is calculated (Figure S7).

Leaf RWC was measured concurrent with RWC_{plant}, according to Sade *et al.* (2015). The leaves used to determine their RWC were picked at 06:00, 10:00 and 14:00 h on 3 days during the drought treatment. The leaf fresh weight (FW) was measured immediately after cutting. Leaf petioles were soaked for 8 h in a 5 mM CaCl solution in a sealed plastic bag, in the dark at room temperature. The turgid weight (TW) was determined after petiole soaking, and the dry weight (DW) was determined after the leaf was dried at 70°C for 72 h. The leaf RWC was then calculated as:

$$\mathrm{RWC}_{leaf} = \left(\frac{\mathrm{FW} - \mathrm{DW}}{\mathrm{TW} - \mathrm{DW}}\right) \cdot 100 \quad (9)$$

The leaf RWC was measured for chosen plants of each line experiencing three similar SWC levels (~80, ~50 and ~20%). Decisions regarding which plants to sample were made before dawn, based on the data collected by the probes continuously monitoring the SWC of each pot.

The leaf area ratio (LAR), defined as the ratio of leaf area (LA) to shoot weight at the end of the experiment ($m^3\ g^{-1}$), and the shoot-weight ratio (SWR), defined as the ratio between the measured shoot weight and the calculated plant weight at the end of the experiment, were calculated for each plant and averaged for plants of the different lines. Plant LA (cm^2) was determined daily by:

$$\mathrm{LA} = \mathrm{PW}*\mathrm{SWR}*\mathrm{LAR} \quad (10)$$

where SWR = 0.6 for both lines. The transpiration rate normalized by plant LA (E [mmol $sec^{-1}\ m^{-2}$]) was equivalent to the values that are usually measured by gas-exchange devices for a small LA. The LA in Eq. 10 refers to the whole plant under examination. The canopy vapor conductance (g_{sc} [mmol $sec^{-1}\ m^{-2}$]) can be calculated using Eq. 6 as:

$$g_{sc} = \frac{\mathrm{WPT} \cdot P_{atm}}{\mathrm{LA} \cdot \mathrm{VPD}} = \frac{E \cdot P_{atm}}{\mathrm{VPD}} \quad (11)$$

where P_{atm} is the atmospheric pressure (101.3 kPa). The VPD, determined as the difference (in kPa) between saturation vapor pressure and actual vapor pressure of ambient air is frequently used to evaluate the atmospheric water demand:

$$\mathrm{VPD} = (1 - \mathrm{RH})0.611 \cdot \exp\left[\frac{17.502 \cdot T}{240.97 + T}\right] \quad (12)$$

where T is the air temperature (°C), RH is the relative humidity (0–1) and 0.611 is the saturation vapor pressure at 0°C; 17.502 and 240.97 are constants (Buck, 1981).

Temporal comparison of the dependence of momentary and cumulative transpiration rate of plants of different cultivars is problematic. The relation of drought time to SWC and its effect on transpiration rate may lead to erroneous conclusions regarding the plant's ability to cope with drought conditions. Plants that transpire more than others will experience lower SWC levels at a given time during drought than those that transpire less. Therefore, the relation between transpiration rate and SWC, rather than time, provides direct information on how different cultivars cope with increasing soil dehydration. The average transpiration rate between 11:00 and 13:00 h was plotted versus SWC for each drought day.

A piecewise linear approximation was then fitted for the different cultivars:

$$E(\theta) = \begin{cases} E_{max} & ;\ \theta \geq \theta_{cr} \\ E_{max} + b(\theta - \theta_{cr}) & ;\ \theta < \theta_{cr} \end{cases} \quad (13)$$

where E_{max}, b, and θ_{cr} are the model-fitting parameters. The piecewise linear approximation is based on Cowan's (1965) hypothesis that transpiration is equal to the lesser of the potential rates representing atmospheric demand, and soil water supply has been widely used in modeling the role of soil moisture on ET (Federer, 1979; Williams and Albertson, 2004 and references therein).

Drought-resistance index (DRI) = $(E_s/E_n)/(M_s/M_n)$; E_s and E_n are the genotype mean transpiration rates under stress and nonstress conditions, respectively, and M_s and M_n are the mean transpiration rates of all genotypes in the given test under stress and nonstress conditions, respectively.

Gas-exchange measurements

Gas-exchange measurements (Figure S4) were taken with a LI-COR 6400 portable gas-exchange system. Analysis was performed on fully expanded M82 leaves grown under the same conditions and at the same time in the same greenhouse as plants in Figure 5. Measurements were taken under saturating light (1200 μmol m^{-2} sec^{-1}; blue light was set to 10% of the photosynthetically active photon) with 400 μmol mol^{-1} CO_2 surrounding the leaf flux density. The leaf-to-air VPD was kept at around 1.5–2.5 kPa during all measurements. Leaf temperature for all measurements was ca. 26°C.

Stomatal aperture and density

Abaxial leaf stomatal aperture and density were imprinted on glass as described by Geisler and Sack (2002). All samples were collected at around 11:00 h. This approach allowed us to reliably score hundreds of stomata from each experiment. In brief, light-bodied vinyl polysiloxane dental resin (Heraeus-Kulzer, http://heraeus-dental.com/) was applied to the abaxial leaf side, dried (~1 min) and removed. The resin epidermal imprints were covered with nail polish, which was removed once it had dried and served as a mirror image of the resin imprint. The nail-polish imprints were placed on microscope slides.

The stomata were counted and photographed under a bright-field inverted microscope (Zeiss 1M7100, Oberkochen, Germany)

on which an HV-D30 CCD camera (Hitachi, Tokyo, Japan) was mounted. Stomatal images were later analyzed to determine aperture size using the ImageJ software (http://rsb.info.nih.gov/ij/) area-measurement tool. The program selection was checked and corrected if necessary for each stomate. A microscope ruler (Olympus, Tokyo, Japan) was used for the size calibration.

Data analysis

All data analyses were performed using Matlab software (MathWorks, Natick, MA, USA). The dataset included daily data (one value per day for each plant) and momentary data acquired every 3 min (480 values per day for each plant). Means that were deemed significantly different at $P < 0.05$ were compared using Student's *t*-test and analysis of variance (ANOVA) (noted in the figure legends). Comparisons of the parameters of Eq. 13 for the two lines were made using 95% confidence intervals. Nonoverlapping confidence intervals indicated a significant difference at $P < 0.05$.

ACKNOWLEDGMENTS

We thank Mr Gil Lerner and Mr Ziv Attia for their practical advice and technical assistance. This study was supported by grant no. OR309/1-1 from the German-Israeli Project Cooperation (DIP).

SUPPORTING INFORMATION

Additional Supporting Information may be found in the online version of this article.

Figure S1. Comparison of whole-plant normalized transpiration and stomatal conductance of M82 and Penelli.

Figure S2. Raw data of the gravimetric system.

Figure S3. Whole-plant transpiration regulation in response to a soil–atmosphere water gradient (winter experiment).

Figure S4. Midday gas-exchange measurements of M82 plants using portable gas-exchange system.

Figure S5. Continuous whole-plant transpiration (ET) and root uptake (J_r) for each individual plant over the course of the day were the soil water content reached ~50%).

Figure S6. Leaf relative water content (RWC) at different levels of soil water content (SWC) levels.

Figure S7. Full treatment growth-profile regime and recovery-rate analysis.

Figure S8. Variation of input voltage and load-cell reading for three constant loads during two typical days.

Table S1. Summary of characteristics of field-grown plants from the literature.

REFERENCES

Bolger, M.E., Weisshaar, B., Scholz, U., Stein, N., Usadel, B. and Mayer, K.F.X. (2014) Plant genome sequencing – applications for crop improvement. *Curr. Opin. Biotechnol.* **26**, 31–37.

Brodribb, T.J. and Holbrook, N.M. (2004) Diurnal depression of leaf hydraulic conductance in a tropical tree species. *Plant Cell Environ.* **27**, 820–827.

Buck, A.L. (1981) New equations for computing vapor pressure and enhancement factor. *J. Appl. Meteorol.* **20**, 1527–1532.

Cowan, I.R. (1965) Transport of water in the soil–plant–atmosphere system. *J. Appl. Ecol.* **2**, 221–239.

Earl, H.J. (2003) A precise gravimetric method for stimulating drought stress in pot experiments. *Crop Sci.* **43**, 1868–1873.

Eshed, Y. and Zamir, D. (1995) An introgression line population. *Genetics.* **141**, 1147–1162.

Federer, C.A. (1979) A soil-plant-atmosphere model for transpiration and availability of soil water. *Water Resour. Res.* **15**, 555–562.

Furbank, R.T. and Tester, M. (2011) Phenomics–technologies to relieve the phenotyping bottleneck. *Trends Plant Sci.* **16**, 635–644.

Geisler, M.J. and Sack, F.D. (2002) Variable timing of developmental progression in the stomatal pathway in Arabidopsis cotyledons. *New Phytol.* **153**, 469–476.

Ghanem, M.E., Marrou, H. and Sinclair, T.R. (2015) Physiological phenotyping of plants for crop improvement. *Trends Plant Sci.* **20**, 139–144.

Golzarian, M.R., Frick, R.A., Rajendran, K., Berger, B., Roy, S., Tester, M. and Lun, D.S. (2011) Accurate inference of shoot biomass from high-throughput images of cereal plants. *Plant Methods*, **7**, 2.

Graff, G., Hochman, G. and Zilberman, D. (2013) The research, development, commercialization, and adoption of drought and stress-tolerant crops. In *Crop Improvement Under Adverse Conditions* (Tuteja, N. and Gill, S.S., eds). New York: Springer, pp. 1–33.

Hartmann, A., Czauderna, T., Hoffmann, R., Stein, N. and Schreiber, F. (2011) HTPheno: an image analysis pipeline for high-throughput plant phenotyping. *BMC Bioinformatics*, **12**, 148. doi:10.1186/1471-2105-12-148.

Hsiao, T.C. and Acevedo, E. (1974) Plant responses to water deficits, water-use efficiency, and drought resistance. *Agric. Meteorol.* **14**, 59–84.

Moshelion, M. and Altman, A. (2015) Current challenges and future perspectives of plant and agricultural biotechnology. *Trends Biotechnol.* **33**, 337–342.

Moshelion, M., Halperin, O., Wallach, R., Oren, R. and Way, D.A. (2014) Role of aquaporins in determining transpiration and photosynthesis in water-stressed plants: crop water-use efficiency, growth and yield. *Plant Cell Environ.* **38**, 1785–1793.

Munns, R., James, R.A., Sirault, X.R.R., Furbank, R.T. and Jones, H.G. (2010) New phenotyping methods for screening wheat and barley for beneficial responses to water deficit. *J. Exp. Bot.* **61**, 3499–3507.

Passioura, J.B. (2012) Phenotyping for drought tolerance in grain crops: when is it useful to breeders? *Funct. Plant Biol.* **39**, 851–859.

Pereyra-Irujo, G.A., Gasco, E.D., Peirone, L.S. and Aguirrezábal, L.A.N. (2012) GlyPh: a low-cost platform for phenotyping plant growth and water use. *Funct. Plant Biol.* **39**, 905–913.

Richards, R.A., Rebetzke, G.J., Watt, M., Condon, A.G. (Tony), Spielmeyer, W. and Dolferus, R. (2010) Breeding for improved water productivity in temperate cereals: phenotyping, quantitative trait loci, markers and the selection environment. *Funct. Plant Biol.* **37**, 85–97.

Sade, N., Vinocur, B.J., Diber, A., Shatil, A., Ronen, G., Nissan, H., Wallach, R., Karchi, H. and Moshelion, M. (2009) Improving plant stress tolerance and yield production: is the tonoplast aquaporin SlTIP2;2 a key to isohydric to anisohydric conversion? *New Phytol.* **181**, 651–661.

Sade, N., Gebretsadik, M., Seligmann, R., Schwartz, A., Wallach, R. and Moshelion, M. (2010) The role of tobacco aquaporin1 in improving water use efficiency, hydraulic conductivity, and yield production under salt stress. *Plant Physiol.* **152**, 245–254.

Sade, N., Galkin, E. and Moshelion, M. (2015) Measuring arabidopsis, tomato and barley leaf relative water content (RWC). *Bio-Protocols*, **5**, 1–4.

Savitzky, A. and Golay, M.J.E. (1964) Smoothing and differentiation of data by simplified least squares procedures. *Anal. Chem.* **36**, 1627–1639.

Taiz, L. and Zeiger, E. (2010) *Plant Physiology, Chapter 3, Water and Plant Cell*. 5th edn. Sunderland, MA: Sinauer Associates, Inc., pp. 80–81.

Topp, G.C., Davis, J.L. and Annan, A.P. (1980) Electromagnetic determination of soil water content: measurements in coaxial transmission lines. *Water Resour. Res.* **16**, 574–582.

Vera-Repullo, J.A., Ruiz-Peñalver, L., Jiménez-Buendía, M., Rosillo, J.J. and Molina-Martínez, J.M. (2015) Software for the automatic control of irrigation using weighing-drainage lysimeters. *Agric. Water Manag.* **151**, 4–12.

Verslues, P.E., Agarwal, M., Katiyar-Agarwal, S., Zhu, J. and Zhu, J.-K. (2006) Methods and concepts in quantifying resistance to drought, salt and freezing, abiotic stresses that affect plant water status. *Plant J.* **45**, 523–539.

Wallach, R., Da-Costa, N., Raviv, M. and Moshelion, M. (2010) Development of synchronized, autonomous, and self-regulated oscillations in transpiration rate of a whole tomato plant under water stress. *J. Exp. Bot.* **61**, 3439–3449.

Williams, C.A. and Albertson, J.D. (2004) Soil moisture controls on canopy-scale water and carbon fluxes in an African savanna. *Water Resour. Res.* **40**, W09302. doi:10.1029/2004WR003208.

Yoo, C.Y., Pence, H.E., Hasegawa, P.M. and Mickelbart, M.V. (2009) Regulation of transpiration to improve crop water use. *Crit. Rev. Plant Sci.* **28**, 410–431.